A Study on the Scalability and Feasibility of the Space-air Integrated Network

Seungwoo Baek and Saewoong Bahk
Department of Electrical and Computer Engineering and INMC, Seoul National University, Seoul, Korea
Email: swbaek@netlab.snu.ac.kr, sbahk@snu.ac.kr

***Abstract*—A key technology in 6G mobile communications is the integration of space and aerial networks. It is a fundamental enabler that provides global coverage for a wide range of applications that require high availability and high resilience. Beyond conceptual system design, many studies discuss how aerial or public networks can efficiently support terrestrial networks. This paper discusses how many users a space-to-air network can serve in an isolated network environment without terrestrial backbone support and which backhaul links are bottlenecks. Based on the recommendation of design parameters of the 3GPP standard, this paper briefly analyzes the path capacity and coverage of a generalized space-to-air network. Through numerical analysis, we confirm that UAV base station altitude is a key factor in improving network performance and supporting close networks.**

I. Introduction

The challenges of the ubiquitous coverage network suggest the importance of the SAGIN (Space-air-ground integrated network). SAGIN has gained prominence recently due to communication satellite and UAV technology advancements. Also, the 3GPP standard [1] accepts NTN (Non-terrestrial network) concepts as future 6G networks, including SAGIN. SAGIN aims to offer seamless coverage and complement each other with each multi-aerial network layer. Based on SAGIN, network providers could establish backhaul links and act as temporary aerial base stations under the vast LEO-SAT (Low Earth Orbit Satellite) constellation supports. UAVs operate at lower altitudes and can provide coverage in localized or rapidly changing areas, addressing communication needs in a dynamic environment. Operating at higher altitudes, HAP covers larger regions in relatively static points, and LEO-SAT offers global coverage. Together, this integration ensures seamless coverage across different spatial scales. However, UAVs have limited endurance time and communication equipment payload limitations, which may impact the range and data throughput. HAPs (High Altitude platforms) face challenges in deployment cost and vulnerability to stratospheric flight control. LEO-SAT can have higher latency, relatively long communication paths, and fast movement on orbital. To address these disadvantages, integrating UAV, HAP, and LEO-SAT in a coordinated manner, as in the SAGIN, can leverage each platform's strengths while mitigating their drawbacks. Numerous studies about SAGIN [2], explicitly explore the synergy and deployment optimization resulting from the strengths and weaknesses of UAV, HAP, and LEO networks. However, to the best of our knowledge, integrated model analyses that

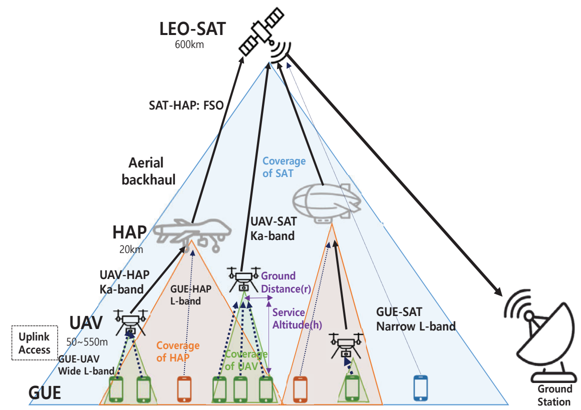

Fig. 1. The concept of the SAGIN with various platforms.

can assess the overall capacity of SAGIN have not yet been presented. In providing an isolated network in vast areas, it becomes imperative to establish a reliable bandwidth threshold that guarantees real-time communication. To analyze multi-hop system link capacity, finding a bottleneck link is essential. For this reason, we evaluate integrated SAGIN performance by examining individual link performance within the general deployment scenario based on the link budget provided by the 3GPP. To evaluate SAGIN performance, we simplified SAGIN service scenarios where each base station supports uplink communication for respective GUE (ground terminals) within the feasible bandwidth as described in Fig. 1. We evaluate the coverage probability of each platform and identify potential bottleneck links. In particular, focusing on UAVs' freely controllable service altitude.

II. System Model and Analysis Methods

We assume GUE, UAV, and HAP are deployed with a 2D PPP probability, each consistently with a density of λ_G,λ_U,λ_H and only a GEO satellite covers entire network area. The GUE first associates with the nearby UAV for uplink. Then, GUE associates with the HAP base station when the access link of the UAV exceeds the threshold SNR θ_{GU}. If the SNR of HAPs the access link is also lower than θ_{GH}, the GUE finally associates the LEO-SAT. Like GUE, UAV determines its association based on whether the SNR of the backhaul link θ_{UH} and HAPs always maintain an association with LEO-SAT. This environment contains six links: GUE-UAV, GUE-

HAP, GUE-SAT, UAV-HAP, and HAP-SAT. UAV altitude h_U determines the LOS (Line of Site) condition of the GUE-UAV link. Also, HAP altitude h_H determines the LOS of the GUE-HAP link. The access link of GUE uses L-band using traditional cellular networks because of size and power limitations. To overcome high path-loss, narrow-band use for HAP and SAT access. UAV are equipped with VSAT (Very Small Aperture Terminals) antennas and use a Ka-band that is used in commercial LEO Internet services. HAP-SAT applies the high-capacity FSO (Free-space optical) backhaul link [3] to support many users' data paths, utilizing its high payloads and power capacity.

A. Coverage Probability

According to Slivnyak's theorem [4], the probability density function (PDF) of the ground projection distance of the GUE-UAS and GUE-HAP links is

$$f(r) = 2\lambda\pi r e^{-\lambda\pi r^2}. \tag{1}$$

and actual link distance $z = \sqrt{r^2 + h^2}$. Following [5], with the neglecting interference based on low SNR conditions and Rayleigh fading channel, the averaged coverage probability of GUE-UAV is

$$\begin{aligned} \mathrm{p}_{GU}(\theta_{GU}, \lambda_U, h_U) &= \int_0^\infty \mathbb{P}(SNR > \theta \mid r) f(r) dr \\ &= \lambda\pi \int_0^\infty 2z e^{-\lambda\pi r - \theta\beta_0\left(\frac{r^2+h^2}{z_0^2}\right)^{\mathbf{g}(h_U)/2}} dz, \end{aligned} \tag{2}$$

where β_0 is the reference SNR value at the distance $d_0 = 100$ [m]. $\mathbf{g}(h)$ is a path-loss exponent of links based on a terrain type that is defined as

$$g(h_U) = \max(\alpha_U - \beta_U h_U + \gamma_U / h_U, 2), \tag{3}$$

where $\alpha_U, \beta_U, \gamma_U$ are suitable terrain parameters for evaluated LOS conditions. Since this path-loss model only applies to low-altitude base stations, we use an approximated model [6] for GUE-HAP links.

$$\begin{aligned} &\varphi_{\mathrm{LOS}} = (1 + (\alpha_H \exp(-\beta_H \left[180/\pi \tan^{-1}(h/z) - \alpha\right])))^{-1} \\ &\mu_{GH} = \varphi_{\mathrm{LOS}} \mu_{\mathrm{GHL}} + (1 - \varphi_{\mathrm{LOS}})\, \mu_{\mathrm{GHN}}, \end{aligned} \tag{4}$$

where α, β is environmental parameters and μ is the mean path-loss of links. In contrast, when r_θ is cell edge distance based on an SNR threshold, we define the probability of HAP links as

$$\mathrm{p}_{\{GH,UH\}}(\theta, \lambda, h) = \int_0^{r_\theta} f(r) dr. \tag{5}$$

According to our assumed association rules, the usage probability Φ of six links could be defined as follows:

$$\begin{cases} \Phi_{GU} = \mathrm{p}_{GU} \\ \Phi_{GH} = \mathrm{p}_{GH}(1 - \mathrm{p}_{GU}) \\ \Phi_{GH} = 1 - \mathrm{p}_{GU} - \mathrm{p}_{GH} + \mathrm{p}_{GU}\mathrm{p}_{GH} \end{cases} \quad \begin{cases} \Phi_{UH} = \mathrm{p}_{UH} \\ \Phi_{US} = 1 - \mathrm{p}_{UH} \\ \Phi_{HS} = 1 \end{cases} \tag{6}$$

B. Average Link Rate

We define the average achievable rate of each link within the coverage area where defined by only a link distance z_θ according to Shannon's theorem and [7] as follows.

$$\begin{aligned} \mathbf{R}_{GU} &= \frac{Bu}{\ln 2} \int_\infty^{\theta_{GU}} \frac{\mathrm{p}\,(\theta, \lambda, h)\,(-10^{(-\theta_{GU}/10)-1} \log 10)}{1 + 10^{\theta_{GU}/10}}\, \mathrm{d}\theta, \\ \mathbf{R}_{\{GS,UH,US\}} &= \frac{Bu}{\ln 2} \int_{z_\theta}^0 \frac{\mathrm{p}\,(\Theta(z), \lambda, h)}{1 + \Theta(z)} \Theta'(z)\, \mathrm{d}z, \end{aligned} \tag{7}$$

where B is the bandwidth of the link, u in the number of channels, and $\Theta'(z)$ is differentiation of Θ that function of SNR of links are

$$\begin{aligned} 10\log_{10}(\Theta_{GU}(z)) &= G_{GU} - \mu_{GH}(z) \\ &\quad - l^R - l^{SN} - l^{FM} - l^I - l^M, \\ 10\log_{10}(\Theta_{\{GS,UH,US\}}(z)) &= G_{\{GS,UH,US\}} - \mu_{\{GS,UH,US\}}(z) \\ &\quad - l^R - l^{NF} - l^{FM} - l^{SC} - l^A - l^M, \\ \mu_{GHL}(z) &= L + 20\log_{10}(f_G) + \sigma_L \log_{10}(z), \\ \mu_{GHN}(z) &= \mu_{GHL}(z) + \kappa \log_{10}(h_O) \\ &\quad - \sigma_N \log_{10}(h_H/z), \\ \mu_{\{GS,UH,US\}}(z) &= L + 20\log_{10}(f_U) + \sigma_L log_{10}(z). \end{aligned} \tag{8}$$

Based on a typical link budget formula, G is the EIRP plus antenna gain ratio to noise temperature. $l^R, l^{SN}, l^{FM}, l^I, l^{SC}, l^A, l^M$ are receiver noise, signal noise figure, fading margin, fixed interference level, scintillation loss, atmospheric loss, and signal demodulation margin respectively. $\sigma_{\{L,N\}}$ is path-loss exponent of LOS/LNOS condition. h_O is average obstacle height and f is carrier frequency. With $\Theta(z)$, we could solve r_θ, z_θ numerically. Meanwhile, according to [8], the capacity of the FSO link could be calculated as follows.

$$\begin{aligned} \mathbf{R}_{HS} &= Buq \log_2[1 + k_1 exp^{-2\omega z_S}], \\ \omega &= \frac{3.91}{V 10^4 \log_{10} e} \left(\frac{f_S}{1550\ [\mathrm{nm}]}\right)^{1.6}, \\ k_1 &= \frac{e^{2\alpha_S \gamma_S}}{2\pi e} \left(\frac{1 - e^{-\gamma_S}}{\gamma_S}\right)^2 \frac{\beta_S^2}{\alpha_S^2}, \end{aligned} \tag{9}$$

where f_S is the wavelength of the transmitter and V is the visibility of the optic signal based on an atmosphere. q is the loss factor related to the satellite's alignment and elevation angle. $\alpha_S, \beta_S, \gamma_S$ is environmental parameters.

Finally, we define achievable capacity per a GUE, Λ, with the assumption of ideally fair resource allocation as follows.

$$\begin{cases} \Lambda_{GU} = \frac{\mathbf{R}_{GU}\lambda_U}{\Phi_{GU}\lambda_G} \\ \Lambda_{GH} = \frac{\mathbf{R}_{GH}\lambda_U}{\Phi_{GH}\lambda_G} \\ \Lambda_{GS} = \frac{\mathbf{R}_{GS}\lambda_U}{\Phi_{GS}\lambda_G} \end{cases} \quad \begin{cases} \Lambda_{UH} = \frac{\mathbf{R}_{GS}\lambda_U}{\Phi_{GS}\Phi_{UH}\lambda_G} \\ \Lambda_{US} = \frac{\mathbf{R}_{US}\lambda_U}{\Phi_{GU}\Phi_{US}\lambda_G} \\ \Lambda_{HS} = \frac{\mathbf{R}_{HS}\lambda_U}{(\Phi_{GU}\Phi_{UH} + \Phi_{GH})\lambda_G} \end{cases} \tag{10}$$

III. Analysis of System Performance

In our analysis, we set the detailed parameter [1], [9] are set as shown in Table I. First, we analyze the GUE and UAV association path ratio according to the coverage

TABLE I
SYSTEM PARAMETERS SETTINGS.

Notations	Settings
$\lambda_G, \lambda_U, \lambda_H / \theta_{GU}, \theta_{\{GH,UH\}}$	75, 1, 1/1600 /km^2 / 0, 13 dB
f_G, f_U, f_S	2, 28 GHz, 550 nm
$B_{\{GU,GH\}}, B_{GS}, B_{\{UH,US\}}, B_{HS}$	10, 0.18, 133, 500 MHz
$\beta_0, G_{GU}, G_{GH}, G_{GS}, G_{UH}, G_{US}, L$	33.8, 42, 18.1, 61.5, 78.2, 32.45 dBm
$l_{GH}^{NF}, l_{GS}^{NF}, l_{\{UH,US\}}^{NF}$	103.1, 146.0, 117.4 dB
$l^{FM}, l_{GH}^{R}, l_{GS}^{A}, l_{GS}^{SC}, l_{UH}^{R}, l_{UH}^{A}, l_{UH}^{SC}$	3, 5, 0.07, 2.2, 1.7, 0.5, 2.2 dB
$l_{US}^{R}, l_{US}^{A}, l_{US}^{SC}, l^{I}, l^{M}$	1.2, 0.5, 0.3, 6, 6 dB
$\alpha_U, \beta_U, \gamma_U, \alpha_H, \beta_H$	4.0, 0.0065, 17.1, 4.88, 0.43
$V, z_S, \alpha_S, \beta_S \gamma_S, q$	50, 580, 0.1, 25, 9.9954, 0.08
$u_{GU}, u_{GH}, u_{GS}, u_{UH}, u_{US}, u_{HS}$	10, 4, 20, 1, 1, 1
$\sigma_L, \sigma_N, \kappa, h_O$	2.0, 3.3, 12, 50

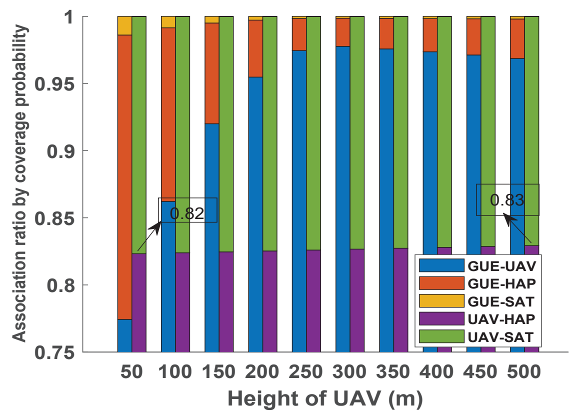

Fig. 2. Link usage ratio from the coverage probability and UAV heights.

probability. Fig. 2 shows that the LOS probability increases the coverage probability of the GUE-UAV together until the altitude of the UAV increases to 300 m. Increasing the UAV altitude to more than 300 m, the path loss GUE-UAV is also increased, and thus, the coverage probability gradually decreases. On the other hand, since HAPs serve at very high altitudes, the probability of usage of a backhaul link does not change significantly due to changes in the altitude of UAVs.

Secondly, we analyze the link capacity occupied by a GUE to identify the general bottleneck link. In Fig. 3., a bottleneck occurs UAV-SAT when the UAV altitude is less than 130 m, as many GUEs share a low-capacity LEO-SAT link. As the altitude of the UAV increases, the UAV-SAT backhaul link gradually becomes saturated. This phenomenon indicates securing high-capacity backhaul in UAV network design is important to reduce bottlenecks. On the other hand, when the density of HAP increases, that is, in an environment where HAPs visit more frequently, the number of GUEs serviced by HAPs increases, making the GUE-HAP link a bottleneck. To mitigate this, UAV needs to increase the service altitude and transfer the load to the GUE-UAV link with a relatively large capacity. In conclusion, UAV base stations at the SAGIN can distribute the load between links by adjusting the UAV altitude, which is an essential factor in determining the system performance experienced by each user.

IV. CONCLUSION

In this paper, we analyze the coverage and link capacity integrated space-air network, one of the essential concepts of

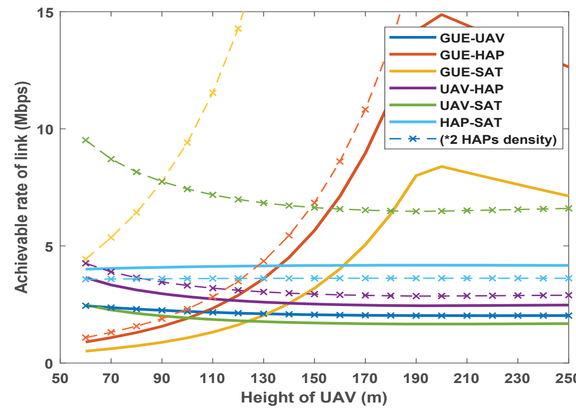

Fig. 3. Achievable access and backhaul link rate by the height of UAV.

6G communication, using realistic parameters. In particular, we focus on finding a bottleneck link not mainly issued by current SAGIN studies but can arise from multi-hop networks. As a result of the system performance analysis, we confirmed that the change in bottleneck links according to the altitude of the UAV base station was an important factor in network design. As part of future work, we will evaluate a practical performance reflecting the mobility of SAT, UAV, and HAP platforms.

ACKNOWLEDGMENT

This research was supported by the MSIT(Ministry of Science and ICT), Korea, under the ITRC(Information Technology Research Center) support program(IITP-2023-2021-0-02048) supervised by the IITP(Institute for Information & Communications Technology Planning & Evaluation)

REFERENCES

[1] 3GPP, "Tr 38.821, solutions for nr to support non-terrestrial networks (ntn)," 2022.

[2] J. Liu, Y. Shi, Z. M. Fadlullah, and N. Kato, "Space-air-ground integrated network: A survey," *IEEE Communications Surveys & Tutorials*, vol. 20, no. 4, pp. 2714–2741, 2018.

[3] R. Samy, H.-C. Yang, T. Rakia, and M.-S. Alouini, "Space-air-ground fso networks for high-throughput satellite communications," *IEEE Communications Magazine*, vol. 60, no. 12, pp. 82–87, 2022.

[4] B. François and B. Bartłomiej, "Stochastic geometry and wireless networks: Volume i theory," *NoW PublishersBreda*, vol. 55, 2009.

[5] L. Zhou, Z. Yang, S. Zhou, and W. Zhang, "Coverage probability analysis of uav cellular networks in urban environments," in *2018 IEEE international conference on communications workshops*, 2018, pp. 1–6.

[6] M. Alzenad, A. El-Keyi, F. Lagum, and H. Yanikomeroglu, "3-d placement of an unmanned aerial vehicle base station (uav-bs) for energy-efficient maximal coverage," *IEEE Wireless Communications Letters*, vol. 6, no. 4, pp. 434–437, 2017.

[7] M. M. Azari, F. Rosas, and S. Pollin, "Cellular connectivity for uavs: Network modeling, performance analysis, and design guidelines," *IEEE Transactions on Wireless Communications*, vol. 18, no. 7, pp. 3366–3381, 2019.

[8] J.-H. Lee, J. Park, M. Bennis, and Y.-C. Ko, "Integrating leo satellites and multi-uav reinforcement learning for hybrid fso/rf non-terrestrial networks," *IEEE Transactions on Vehicular Technology*, vol. 72, no. 3, pp. 3647–3662, 2022.

[9] D. Wang, M. Giordani, M.-S. Alouini, and M. Zorzi, "The potential of multilayered hierarchical nonterrestrial networks for 6g: A comparative analysis among networking architectures," *IEEE Vehicular Technology Magazine*, vol. 16, no. 3, pp. 99–107, 2021.